Time-dependent screening in the electron gas

G. S. Canright
Solid State Division, Oak Ridge National Laboratory, Oak Ridge, Tennessee 37831
and Department of Physics, University of Tennessee, Knoxville, Tennessee 37916
(Received 22 June 1987; revised manuscript received 4 December 1987)

The transient screening response in real space and time of the electron gas to a suddenly created point charge is calculated in the linear approximation, in a way which allows the decomposition of the response into a part due to plasmons and a part due to electron-hole pairs. The results are expected to be qualitatively correct as a description of core-hole creation in simple metals in the limit of large photoelectron energies. We obtain a clear picture of an electronic "shock wave" which propagates outward from the core hole with some dispersion; the group velocities are centered at the Fermi velocity. Behind the shock wave is the static distribution plus a small ringing due to small-q plasmons. The results are examined in the light of experimental evidence for transient effects on core-hole decay.

I. INTRODUCTION

The screening response of conduction electrons plays an important role in nearly all physical behavior in metals. Hence the characterization of metallic screening has received considerable attention and effort. The point impurity is a commonly treated perturbation, due both to its tractability and to its suitability for a variety of physical problems, including hydrogen in metals,[1-3] positron annihilation,[4,5] moving charged ions,[6,7] NMR spectra,[8] and soft-x-ray-absorption (SXA) and -emission (SXE) spectra.[9]

The majority of the work on the point impurity applies to the static limit. Static screening calculations include those restricted to the linear approximation,[7,8,10,11] and those going beyond it,[1-6,9] which commonly employ density-functional theory[12] or a variant. Dynamic calculations, on the other hand, tend to be restricted to the linear approximation[7,13]; a suitable nonlinear theory remains to be developed, although some steps have been taken in this direction.[14,15]

The problem of metallic x-ray spectra is a particularly interesting transient screening problem. When an x ray is absorbed by an ionic core in a metal, a variety of processes occur at various time scales; included in these are the reaction of the sea of conduction electrons, i.e., the screening. Part of the x-ray energy is imparted to a photoelectron which is ejected from the core; it leaves the vicinity of the remaining core hole in a time τ_e which depends on its energy. The remaining core electrons relax in the presence of the hole in a time τ_{ce}; the conduction electrons screen both the core hole and the photoelectron with some characteristic time τ_{sc}. We will assume, based on the large discrepancy in energy scales, that $\tau_{ce} \ll \tau_{sc}$.

The electron departure time τ_e can vary widely, depending on the energy of the incoming photon. For a highly energetic photon, the photoelectron velocity is very large, and $\tau_e \to 0$; while, as the photon energy approaches the threshold for core ionization, $\tau_e \to \infty$. The theory of x-ray spectra at threshold, due to Mahan[16] and Nozières and DeDomenicis[17] (MND), thus takes $\tau_{sc}/\tau_e = 0$, i.e., it assumes instant screening of the core hole. Farther from threshold one uses the "final-state rule," a one-particle formalism, to calculate spectra[18-20]; this theory also neglects the dynamics of screening. Gadzuk and Sunjić have developed a theory[21] for photoelectron spectra [x-ray photoelectron spectroscopy (XPS)] which spans the range $0 \lesssim \tau_e < \infty$, but which again is based on $\tau_{sc} \simeq 0$.

In contrast to the above work, there have been a number of attempts to calculate the effects of screening transients on x-ray spectra. Persistent transients in the electron gas should be detectable in the spectra generated by the subsequent decay of the core hole, either by Auger-electron emission (at a time τ_A) or by x-ray emission (radiative decay, τ_r). Coupling of the emission process to screening transients should produce structure in the resulting spectrum *above* the threshold energy, as well as possibly detectable effects on the spectrum below threshold. Yue and Doniach[22] have demonstrated the effect of screening transients in the high-energy tail of SXE spectra, while several authors[23-25] have examined the more prominent "plasmon-gain" structure seen in Auger-electron spectra (AES). At the other end of the spectrum, Minnhagen[26] and Shung and Langreth[27] have shown that the threshold theory for XPS spectra may be applied within a plasmon energy from threshold, if dynamic screening is properly incorporated.

Finally, we mention the theoretical work of Noguera, Spanjaard, and Friedel.[13] They gave the photoelectron a classical (constant) velocity $\mathbf{v}$ and then used linear-response theory, in the plasmon-pole approximation, to find the response of the electron gas to the two perturbing point charges,

$$\rho_{ext}(\mathbf{r},t) = e\Theta(t)[\delta(\mathbf{r}) - \delta(\mathbf{r}-\mathbf{v}t)] , \quad (1)$$

where the first term is the core hole and $\Theta(t)$ is the step

function. This semiclassical model thus incorporates both dynamic screening and a wide range of τ_e (by varying $|\mathbf{v}|$), although clearly the classical picture of the electron velocities $\mathbf{v}$ fails as $\mathbf{v}\to\mathbf{0}$. They have applied the model to the high-energy range of x-ray absorption, i.e., to EXAFS (extended x-ray-absorption fine structure).[28]

The present work is an attempt to accurately characterize the screening transients associated with the creation of a core hole in a metal. In keeping with the current state of the theory we restrict ourselves to the linear-screening approximation. We also make two common approximations: that there is no spatial or temporal structure to the core hole, and that the metal may be modeled as jellium. We choose a compromise somewhat different from that of Noguera, Spanjaard, and Friedel; however, we take the $\tau_e\to 0$ limit, while employing the full (linear) dielectric function. Thus we treat, in linear response, the space and time dependence of the screening-charge response to the perturbing charge,

$$\rho_{\text{ext}}(\mathbf{r},t)=e\delta(\mathbf{r})\Theta(t)\ . \tag{2}$$

It is in this (sudden) limit that the photoelectron is completely decoupled from subsequent transients. Computationally, this means we treat a monopole rather than a dipole. Physically, one expects the appearance of only those transients whose rate (energy) is smaller than that of the photoelectron (τ_e^{-1}); thus we sample the full spectrum in the $\tau_e=0$ limit. It is just this limit (of a highly energetic photoelectron) in which one expects to see effects of persistent transients appearing in subsequent emission spectra.[22–25] Hence we may expect to gain some insight into these effects from examining these transients in the sudden limit.

II. THEORY

In linear-response theory

$$\rho_t(\mathbf{q},\omega)=\rho_{\text{ext}}(\mathbf{q},\omega)+\rho_s(\mathbf{q},\omega)=\frac{\rho_{\text{ext}}(\mathbf{q},\omega)}{\epsilon(\mathbf{q},\omega)}\ ,$$

or

$$\rho_s(\mathbf{q},\omega)=\rho_{\text{ext}}(\mathbf{q},\omega)\left[\frac{1}{\epsilon(\mathbf{q},\omega)}-1\right]\ , \tag{3}$$

where ρ is a charge density, $\epsilon(\mathbf{q},\omega)$ is the dynamic dielectric function, and the subscripts t, ext, and s refer to "total," "external," and "screening," respectively.

The Fourier transform of (2) gives

$$\rho_{\text{ext}}(\mathbf{q},\omega)=\frac{i}{\omega+i\delta}\ , \tag{4}$$

where δ is a positive infinitesimal and we have let e (the electronic charge) = 1.

Substituting (4) into (3) and taking the inverse transform, we get, after some manipulation (see Appendix),

$$\rho_s(r,t)=\frac{1}{\pi^3 r}\Theta(t)\int_0^\infty dq\ q\ \sin qr \times\int_0^\infty\frac{d\omega}{\omega}\left[\text{Im}\left[\frac{1}{\epsilon(q,\omega)}\right]\right]\times(1-\cos\omega t)\ . \tag{5}$$

The spectral function $\text{Im}(1/\epsilon)$ consists of a continuum part, representing e-h-pair excitations, and a plasmon peak for certain values ω_q.[29] Hence we can find the separate contributions to ρ_s from each type of excitation (See Appendix):

$$\rho_s^{e\text{-}h}=\frac{\Theta(T)}{\pi^3 R}\int_0^\infty Q\,dQ\,\sin QR \times\int_{\Omega_1}^{\Omega_2}\frac{d\Omega}{\Omega}\left[\text{Im}\left[\frac{1}{\epsilon(Q,\Omega)}\right]\right]\times[1-\cos(\alpha'\Omega T)]\ , \tag{6}$$

$$\rho_s^{p}=\frac{-\Theta(T)}{\pi^2 R}\int_0^{Q_c} Q\,dQ\,\sin QR\left[\frac{1-\cos(\alpha'\Omega_Q T)}{\Omega_Q\,|\,\epsilon_1'\,|\,\Omega_Q}\right]\ . \tag{7}$$

Here we have changed to dimensionless quantities:

$$Q=q/k_F,\quad R=k_F r,\quad T=\omega_p t,\quad \Omega=\omega/E_F\ ,$$

where k_F is the Fermi wave vector, ω_p is the long-wavelength plasma frequency, and E_F is the Fermi energy. The charge densities are scaled to k_F^3. Now we take

$$\epsilon(q,\omega)=1-\frac{v_q P(q,\omega)}{1+v_q G(q)P(q,\omega)}\ , \tag{8}$$

where v_q is the Fourier transform of the Coulomb potential, $P(q,\omega)$ is the Lindhard function,[30] and $G(q)$ is the (static) local-field correction to the random-phase approximation (RPA).[31] Using (8), we can numerically integrate (6) and (7) to find the two charge densities.

III. RESULTS

For the function $G(q)$ in Eq. (8) we have used two choices: $G=0$ (RPA) and a parametrized version due to Vashishta and Singwi,[32] $G=G_{\text{VS}}(q)$. Other parametrized versions for $G(q)$ are available[33]; however, since the results for $G=0$ and for $G=G_{\text{VS}}$ differ only slightly, these other choices were not explored.

The electron density is reflected in the parameter r_s, which is small for high densities. We chose a typical metallic density, $r_s=3$ (close to Li at $r_s=3.24$). A limited examination was also carried out for a low-density case, $r_s=6$.[34]

As a check we have calculated the static charge distribution by omitting the cosine term in Eqs. (6) and (7). The results, when summed, were identical to those obtained previously[10,32] for the same G and r_s; however, the decomposition has not previously been obtained. The results for the RPA and $r_s=3$ are shown in Fig. 1; each component is multiplied by $4\pi R^2$. Figure 1 reveals the standard Friedel oscillations at large R, but only in the net density. What we find is that the partitioning of the

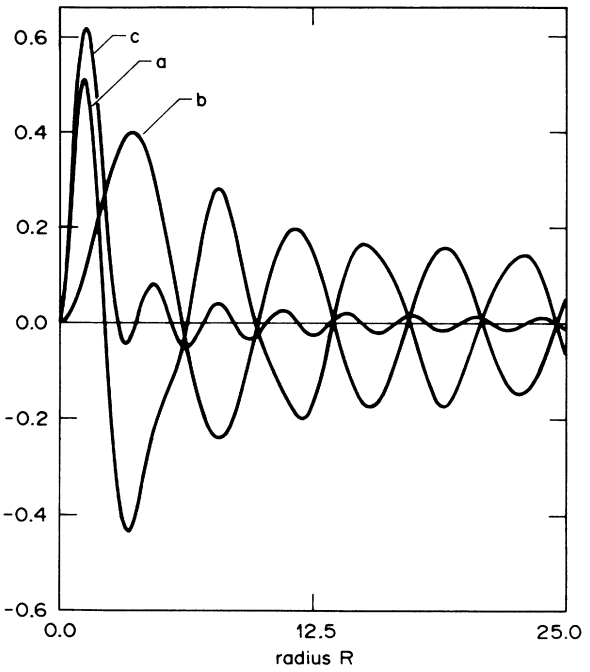

FIG. 1. The static screening density for a point charge at the origin, decomposed into *a*, a part due to continuum (*e-h*) excitations; *b*, a part due to plasmons; and *c*, total. Radial units are $R=k_F r$; densities are normalized to k_F^3 (where k_F is the Fermi wave vector) and multiplied by $4\pi R^2$.

spectral density introduces singularities in the integrands, and hence oscillations in the component densities, which mask the weak $2k_F$ singularity responsible for the Friedel oscillations. Hence the separate components (plasmon and *e-h*) had to be calculated quite accurately at large R.

In Figs. 2–4 we show the time development of the three densities $\rho^{e\text{-}h}$, ρ^p, and $\rho^t=\rho^{e\text{-}h}+\rho^p$ in the RPA for $r_s=3$. In each case the density (scaled to k_F^3) is again multiplied by $4\pi R^2$ so as to clarify the large-R behavior.

We see from Figs. 2–4 that the partitioning of the response into plasmon and quasiparticle components is somewhat illuminating but also unphysical. The *e-h* part clearly retains plasmonlike spectral weight, which, in contrast to the plasmon part, loses phase coherence at large times. We also notice that the small-R density is dominated by the *e-h* component, which builds rapidly ($\omega_p t \simeq 1$–2) to its static value; the plasmon part merely adds a small, lightly damped ringing to this peak.

The unphysical aspect is revealed by the large amplitudes in Figs. 2 and 3 at large R and small T, which are totally absent in Fig. 4, the physical density. Disturbances in the gas propagate at a group velocity $v_g \simeq v_F$, the Fermi velocity, which is ≈ 1 in the units of Fig. 4.

We can, in fact, estimate the dispersion in the "shock wave" which is revealed in Fig. 4. As may be seen in the figure, the leading component of the wave propagates at $v_{g1} \simeq (2-3)v_F$. We also find (which is obscured in Fig. 4) that a trailing edge may be defined, such that, behind the trailing edge, we find essentially the static distribution. A plot of the position of this edge between $T=\pi$ and 8π gives it velocity as $v_{g2} \simeq 0.2 v_F$, an order of magnitude

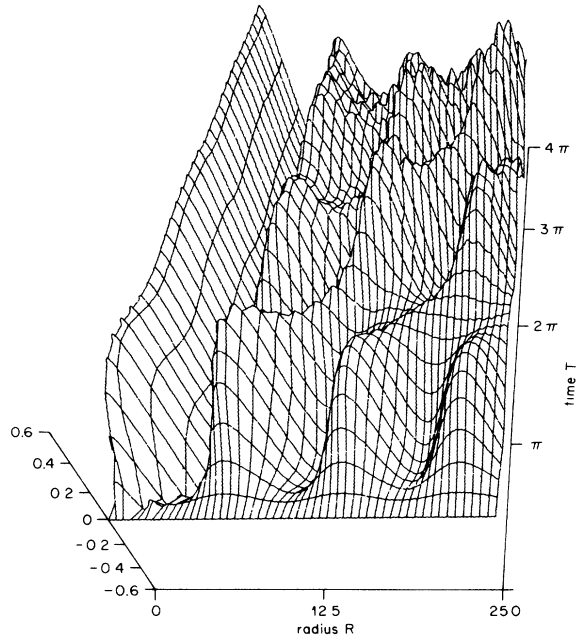

FIG. 2. Time dependence of the *e-h* part of the screening density, in units of Fig. 1, with time $T=\omega_p t$, where ω_p is the plasma frequency. Note the rapid buildup at small R and the loss of coherence at large R.

lower. Hence the wave has significant dispersion, although the bulk of the energy propagation is centered at v_F.

Finally, we must point out that the small-T segment of our calculation necessarily fails to be totally realistic in neglecting the photoelectron, whose velocity has an

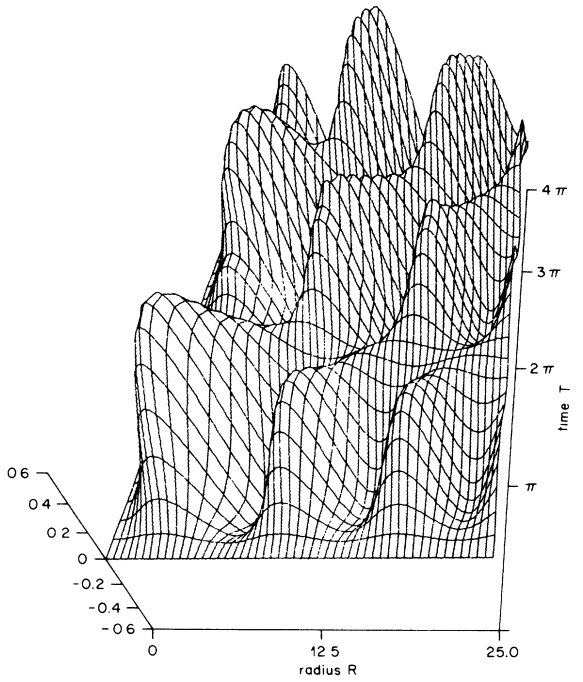

FIG. 3. Time dependence of the plasmon part; units as in Fig. 2. The plasmons propagate coherently but are not large at small R.

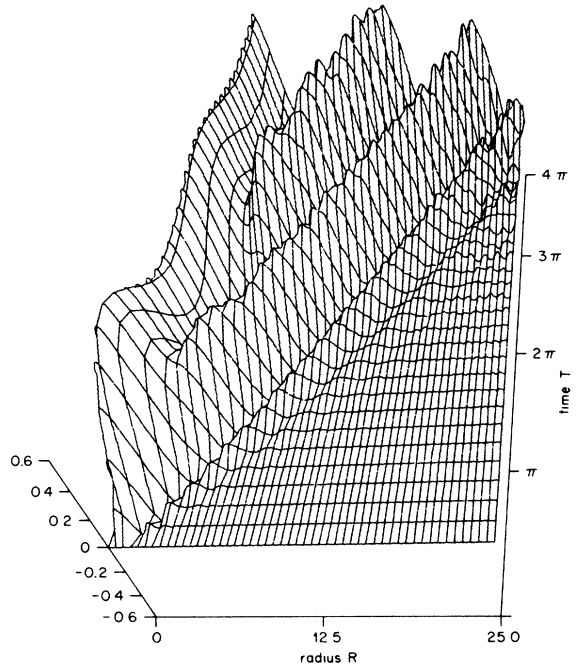

FIG. 4. Time dependence of the net screening density, i.e., the sum of Figs. 2 and 3. The unphysical amplitudes at large R and small T have canceled, leaving a clear picture of a propagating electronic shock wave.

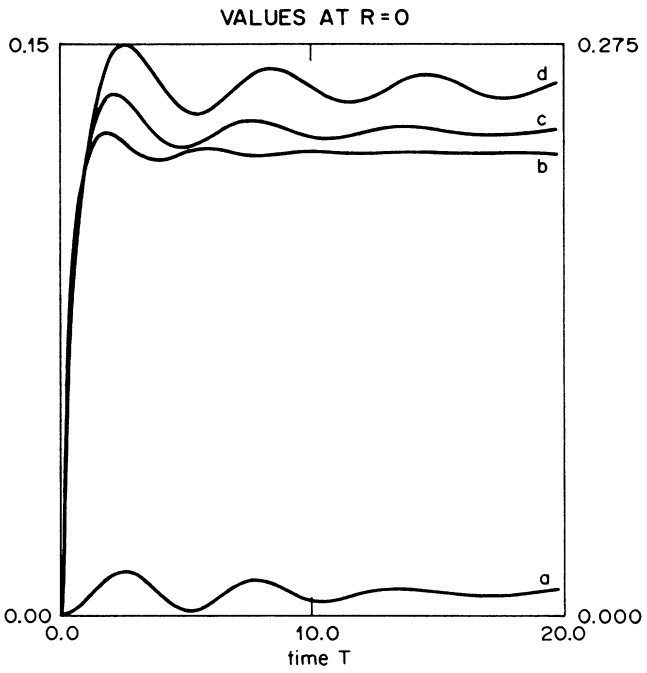

FIG. 5. Densities at $R=0$ as a function of time: *a*, plasmon part, RPA, $r_s=3$; *b*, *e-h* part, RPA, $r_s=3$; *c*, net screening density, RPA, $r_s=3$ [(a) + (b)]; *d*, net screening density, $G=G_{\rm VS}$, $r_s=6$. Units are as in previous figures, except that densities are not multiplied by $4\pi R^2$. Left-hand scale is for *a*–*c*; right-hand scale, *d*. The plasmon part is small, but provides most of the long-term transient; this effect is enhanced for the case *d*.

upper bound ($c\approx 300$ in our units) regardless of its energy. For example, a 2.5-keV electron has $v\sim 0.1c\sim 30$, which places it at $R\sim 12$ for $T=\pi/8$, and its "wake" (Ref. 7) would persist for longer times. Hence our sudden approximation requires for its validity not only large photoelectron energies but a restriction to times not too close to zero as well.

Figure 5 shows charge densities at the origin as a function of time; these quantities are invisible due to the $4\pi R^2$ scaling in Figs. 2–4. The results agree with the qualitative conclusions obtained for the small-R portion of Figs. 2–4: The density at $R=0$ is dominated by the fast-rising, heavily damped *e-h* part, which reaches its steady value at $T\simeq 1$–2. The additional plasmon ringing is on the order of 5% of the total amplitude at the origin. This ringing is more pronounced ($\lesssim 10\%$) for the case $r_s=6$ and $G=G_{\rm VS}$, also shown in Fig. 5; other cases were intermediate.

Figure 5 reveals that, strictly, $v_{g2}=0$, since there is a finite persistent transient at $R=0$ for all times. Hence the "essentially" static distribution described above (behind the trailing edge of the wave front) actually includes a persistent ringing similar to that of Fig. 5, around the static configuration (Fig. 1).

We have also calculated and plotted the integrated charge $Z(R,T)$ for the three densities, defined as

$$Z_i(R,T)=\int_0^R dR'4\pi(R')^2\rho^i(R'T),\quad i=e\text{-}h,p,t\ .$$

However, the results can be described analytically and hence are not shown here. We find that, for $R\to\infty$,

$$Z_{e\text{-}h}(\infty,T)=0\ , \tag{9a}$$

$$Z_p(\infty,T)=Z_t(\infty,T)=1-\cos T\ . \tag{9b}$$

That is, all the net screening charge is contained in the plasmon part, which, in turn (for an infinite solid), possesses no steady-state limit. The former result stems from the fact that $Z_t(\infty,T)$ selects the $Q=0$ portion of the spectral density, which is entirely accounted for by plasmons.[29] The latter conclusion depends on the lack of damping of $Q=0$ plasmons in the jellium model, and on the infinite size of the solid. Any damping of these plasmons due to band-structure effects[35] will drive the $\cos T=\cos\omega_p t$ term to zero in Eq. (9b), giving the proper charge $Z_t(\infty,\infty)=1$, which was obtained in our static calculation.

IV. DISCUSSION

We recall the physical problem under consideration: the creation of a core hole, and its subsequent decay. Clearly, the above results give a description of the environment the core hole sees at the time of decay, and perhaps some insight into the physics involved.

First, we consider Auger decay. A typical time for Auger decay[36] is $\tau_A\simeq 20$ ($t_A\simeq 20\omega_p^{-1}$). At $T=20$ we have essentially static screening out to $R\simeq 4$, which is about 3 Å—a nearest-neighbor distance.

Again, "essentially" implies that any persistent ringing is $\lesssim 1\%$. Hence the emitting core hole at time τ_A is surrounded by a weakly ringing but nonpropagating screening cloud, beyond which is a propagating shell of transients in a dispersive spherical wave. Effects of screening transients on the emitted Auger electron may thus arise from either the weak local ringing, or from the disturbance propagating in the bulk. The former origin appears more probable in the light of the extent of the propagating shell, but the picture is more complex in real solids, due to the presence of (a) a surface which cannot be far from the emitting core hole, and (b) propagating disturbances from other core holes in the solid.

For radiative emission we have that $\tau_r \gg \tau_A$. However, those photons which are emitted and detected have competed successfully with Auger processes, so we take $\tau_r \simeq \tau_A$. Thus the environment most probably present at the time of radiative emission is that described above. Experimentally, we find in this case some evidence for a small *e-h* enhancement of the emission edge due to persistent transients, but no plasmon-gain peak.[22] Clearly, the real-space picture of screening obtained here, while complementing the numerous studies in q and ω space, is insufficient to address the observed difference between Auger and SXE plasmon-gain structures; this question has been treated by Langreth.[37] Our R- and T-space picture may be useful in explaining measurements made in real space and time; at this time we are aware of none connected with core-hole creation in metals.

Finally, we mention a recent experiment[38] which has apparently indirectly measured the kind of electronic shock wave which we have described above. Brorson *et al.* applied pulsed-laser excitation to one face of a thin metallic film and found that the resulting disturbance propagated through the film with $v_g \simeq v_F$; they also noted some dispersion in the propagation. Neither of these features is surprising in the light of our results.

In conclusion, we have calculated the transient-screening response to a suddenly created point charge in jellium. Our method allows the decomposition of the response into a part due to plasmons and a part due to quasiparticle-pair excitations. We have found that a spherical electronic shock wave propagates outward from the impurity in a dispersive fashion, with a range of velocities centered at the Fermi velocity v_F. Behind this wave remains a charge distribution composed of the static screening charge plus a weak ringing due to plasmons. At typical Auger- or x-ray-emission times, the bulk of the transients have propagated away from the core hole, as expected from simple estimates.[22,25] We note evidence that a similar shock wave has been detected experimentally.[38]

ACKNOWLEDGMENTS

Thanks are due to G. D. Mahan for suggesting the problem, and for a simplification of the derivation. Helpful conversations with T. A. Callcott, J. Burgdörder, G. Vignale, and D. Zimmerman are grateful acknowledged. Research support is acknowledged from the University of Tennessee and from the Division of Materials Science, U. S. Department of Energy (through the Oak Ridge National Laboratory, operated by Martin Marietta Energy Systems, Inc., under Contract No. DE-AC05-840R21400).

APPENDIX

This appendix contains details of the derivations in Sec. II. We drop the vector notation in $\epsilon(q,\omega)$ as there is no angular dependence; then, inserting (4) into (3) and double transforming gives

$$\rho_s(r,t)=\frac{1}{4\pi^3 r}\int_0^\infty dq\, q \sin qr \int_{-\infty}^{\infty} d\omega\, e^{-i\omega t}\left[\frac{1}{\epsilon(q,\omega)}-1\right]\left[\frac{i}{\omega+i\delta}\right]. \tag{A1}$$

Next we note that

$$B(q,\omega)=B_1(q,\omega)+iB_2(q,\omega)=\left[\frac{1}{\epsilon(q,\omega)}-1\right]$$

has the required properties for the Kramers-Kronig relations.[29] So we have that

$$B(q,\omega)=-\frac{1}{\pi}\int_{-\infty}^{\infty} d\omega' \frac{B_2(q,\omega')}{\omega-\omega'+i\delta},$$

which combined with (A1) gives

$$\rho_s(r,t)=\frac{1}{4\pi^3 r}\int_0^\infty dq\, q \sin qr \int_{-\infty}^{\infty} d\omega' B_2(q,\omega')\left[\frac{-i}{\pi}\int_{-\infty}^{\infty} d\omega \frac{e^{-i\omega t}}{(\omega+i\delta)(\omega-\omega'+i\delta)}\right].$$

Contour integration gives the quantity in large parentheses as

$$2\left[\frac{1-e^{-i\omega' t}}{\omega'}\right]\Theta(t),$$

so that

$$\rho_s(r,t)=\frac{1}{2\pi^3 r}\Theta(t)\int_0^\infty dq\, q\,\sin qr\int_{-\infty}^{\infty}\frac{d\omega}{\omega}B_2(q,\omega)(1-e^{-i\omega t})\ . \tag{A2}$$

Equation (5) results from (A2) and the fact that $B_2(q,\omega)$ is an odd function of ω.

In Eqs. (6) and (7), ω_q is defined by

$$\epsilon_1(q,\omega_q)=0 \quad \text{and} \quad \epsilon_2(q,\omega_q)=0\ ,$$

$$\omega_p=\lim_{q\to 0}\omega_q$$

(i.e., the long-wavelength plasma frequency), Ω_Q is defined analogously to ω_q,

$$\alpha'=\frac{\alpha^2}{(12r_s)^{1/2}},\quad \alpha=\left[\frac{9\pi}{4}\right]^{1/3},$$

and r_s is a dimensionless quantity defined by[29]

$$\tfrac{4}{3}\pi(r_s a_0)^3=\frac{1}{n_0}\ ,$$

where n_0 is the uniform unperturbed density of the electron gas, and a_0 is the Bohr radius,

$$\Omega_1=\max(0,\ Q^2-2Q)\ ,$$

$$\Omega_2=Q^2+2Q\ ,$$

$$|\epsilon_1'|_{\Omega_Q}=\left|\frac{d\epsilon_1(Q,\Omega)}{d\Omega}\right|_{\Omega=\Omega_Q}.$$

The limits on the Ω integral in (6) are the upper and lower bounds for the e-h continuum. To get (7), we note that

$$\lim_{\epsilon_2\to 0}B_2=-\pi\delta(\epsilon_1)=\frac{-\pi\delta(\Omega-\Omega_Q)}{\left|\dfrac{d\epsilon_1(Q,\Omega)}{d\Omega}\right|_{\Omega=\Omega_Q}}\ .$$

The upper limit (Q_c) in (7) is the point at which the plasmon curve meets the e-h continuum, i.e.,

$$Q_c^2+2Q_c=\Omega_{Q_c}\ .$$

Finally, we can recover the steady-state result for ρ_s from (5) as follows. For $t\to\infty$, the term $\cos(\omega t)$ will integrate to zero. Hence,

$$\rho_s(r,\infty)=\frac{1}{2\pi^3 r}\int_0^\infty dq\, q\,\sin qr\int_{-\infty}^{\infty}\frac{d\omega}{\omega}B_2(q,\omega)$$

[cf. Eq. (A2)]. Since the residue of B_2 is zero at $\omega=0$, the ω integral is equal to its principal part. Then a Kramers-Kronig transformation gives

$$\rho_s(r,\infty)=\frac{1}{2\pi^2 r}\int_0^\infty dq\, q\,\sin qr B_1(q,0)$$

$$=\frac{1}{2\pi^2 r}\int_0^\infty dq\, q\,\sin qr\left[\frac{1}{\epsilon(q,0)}-1\right]. \tag{A3}$$

The standard result[11] is Eq. (A3) multiplied by -1 to convert negative (electronic) charge densities to positive particle densities. We have done the same.

[1] C. O. Almbladh, U. von Barth, Z. D. Popovic, and M. J. Stott, Phys. Rev. B **14**, 2250 (1976).

[2] J. K. Nørskov, Phys. Rev. B **20**, 446 (1979).

[3] P. Jena and K. S. Singwi, Phys. Rev. B **17**, 3518 (1978).

[4] A. Sjölander and M. J. Stott, Phys. Rev. B **5**, 2109 (1972).

[5] P. Bhattacharyya and K. S. Singwi, Phys. Rev. Lett. **29**, 22 (1972).

[6] N. Barberan and P. M. Echenique, J. Phys. B **19**, L81 (1986); P. M. Echenique, R. M. Nieminen, and R. H. Ritchie, Solid State Commun. **37**, 779 (1981).

[7] A. Mazarro, P. M. Echenique, and R. H. Ritchie, Phys. Rev. B **27**, 4117 (1983).

[8] G. Grüner and M. Minier, Adv. Phys. **26**, 231 (1977).

[9] G. W. Bryant and G. D. Mahan, Phys. Rev. B **17**, 1744 (1978).

[10] J. S. Langer and S. H. Vosko, J. Phys. Chem. Solids **12**, 196 (1959).

[11] K. S. Singwi and M. P. Tosi, Phys. Rev. **181**, 784 (1969); K. S. Singwi, A. Sjölander, M. P. Tosi, and R. H. Land, Phys. Rev. B **1**, 1044 (1970).

[12] P. Hohenberg and W. Kohn, Phys. Rev. **136**, B864 (1964); W. Kohn and L. J. Sham, *ibid.* **140**, A1133 (1965).

[13] C. Noguera, D. Spanjaard, and J. Friedel, J. Phys. F **9**, 1189 (1979).

[14] E. Runge and E. K. U. Gross, Phys. Rev. Lett. **52**, 997 (1984); E. K. U. Gross and W. Kohn, *ibid.* **55**, 2850 (1985).

[15] S. C. Ying, Nuovo Cimento B **23**, 270 (1974); G. Mukhopadhyay and S. Lundqvist, *ibid.* **27**, 1 (1975).

[16] G. D. Mahan, Phys. Rev. **163**, 612 (1967).

[17] P. Nozières and C. T. DeDomenicis, Phys. Rev. **178**, 1097 (1969).

[18] U. von Barth and G. Grossmann, Solid State Commun. **32**, 645 (1979); Phys. Rev. B **25**, 5150 (1982).

[19] G. D. Mahan, Phys. Rev. B **21**, 1421 (1980).

[20] L. C. Davis and L. A. Feldkamp, Phys. Rev. B **23**, 4269 (1981).

[21] J. W. Gadzuk and M. Sŭnjić, Phys. Rev. B **12**, 524 (1975).

[22] J. T. Yue and S. Doniach, Phys. Rev. B **8**, 4578 (1973).

[23] C. O. Almbladh, Nuovo Cimento B **23**, 75 (1974).

[24] J. C. Fuggle, R. Lässer, O. Gunnarsson, and K. Schönhammer, Phys. Rev. Lett. **44**, 1090 (1980); O. Gunnarsson, K. Schönhammer, J. C. Fuggle, and R. Lässer, Phys. Rev. B **23**, 4350 (1981).

[25] K. W. K. Shung and D. C. Langreth, Phys. Rev. B **28**, 4976 (1983).

[26] P. Minnhagen, J. Phys. F **7**, 2441 (1977).

[27] K. Shung and D. C. Langreth, Phys. Rev. B **23**, 1480 (1981).

[28] C. Noguera and D. Spanjaard, J. Phys. F **11**, 1133 (1981).

[29] G. D. Mahan, *Many-Particle Physics* (Plenum, New York, 1983).

[30] J. Lindhard, K. Dan. Vidensk. Selsk. Mat.-Fys. Medd. **28**, No.

1 (1954).
[31]S. Ichimaru, Rev. Mod. Phys. **54**, 1017 (1982).
[32]P. Vashishta and K. S. Singwi, Phys. Rev. B **6**, 875 (1982).
[33]K. S. Singwi, A. Sjölander, M. P. Tosi, and R. H. Land, Phys. Rev. Rev. B **1**, 1044 (1970); K. Utsumi and S. Ichimaru, Phys. Rev. A **26**, 603 (1982); I. Nagy, J. Phys. C **19**, L481 (1986). M. Mostoller (unpublished) has obtained an analytic expression for the local-field correction of D. J. W. Geldart and R. Taylor [Can. J. Phys. **48**, 167 (1970)].
[34]For $G=G_{VS}$ (and for most other theories besides the RPA) the value $r_s=6$ is somewhat beyond the stability limit for the electron gas, i.e., the compressibility becomes negative (Ref. 29).
[35]P. C. Gibbons, Phys. Rev. B **17**, 549 (1978), and references therein.
[36]P. H. Citrin, G. K. Wertheim, and Y. Baer, Phys. Rev. B **16**, 4526 (1977).
[37]D. C. Langreth, Phys. Rev. Lett. **26**, 1229 (1971).
[38]S. D. Brorson, J. G. Fujimoto, and E. P. Ippen, Phys. Rev. Lett. **59**, 1962 (1987).